

# TRANSIENTS AND MASS EJECTIONS OBSERVED IN RADIO OCCULTATION MEASUREMENTS OF THE SOLAR CORONA

Richard Woo

Jet Propulsion Laboratory, California Institute of Technology

Pasadena, California 91109

**Abstract** A wide variety of radio propagation and scattering phenomena observed when a radio source is occulted by the solar corona has formed the basis for probing the solar corona for over four decades. The purpose of this paper is to review the subject of transients — variations in the radio occultation measurements that appear different from those of the background solar wind. A major surprise in the study of transients has been the realization that they can represent the passage of coronal streamers in addition to the coronal mass ejections (CMEs) observed in white-light coronagraphs. Although common radio occultation and white-light measurements of CMEs have been few and incomplete, some general features of CMEs are emerging.

Two regions of enhanced density and density fluctuations appear common to CMEs. The first represents the compressed plasma ahead of the CME, and is present whether or not the CME is traveling fast enough to generate an interplanetary shock, while the second corresponds to the bright core of the CME observed in white-light. Polarity reversals, presumably due to the deflection of the magnetic field by the advancing CME, occur behind the compressed plasma. As in the case of CMES observed by in situ measurements and identified as **counterstreaming superthermal** electrons events, polarity reversals are not always observed in the white-light CMEs. Multiple polarity reversals in the body of the CME are suggestive of large internal field rotations, magnetic flux ropes, and magnetic cloud. These coronal features of CMES are consistent with their interplanetary manifestation as observed by in situ measurements of the solar wind at 1 AU.

## 1. INTRODUCTION

Imagine a white-light coronagraph whose field of view extends to 1 AU, yielding precise, high sensitivity and high time resolution measurements of polarization brightness, but only at one point in the plane of the sky. Or, imagine a spacecraft in the corona, instrumented to make solar wind measurements integrated along a linear path that includes the spacecraft and Earth. Measured — not necessarily all the time, and certainly not simultaneously — are: (1) density with high precision, high sensitivity, and high time resolution, (2) solar wind velocity with lower precision and higher uncertainty, and (3) the product of density and the component of magnetic field along the path. Imagine again, farther away from the Sun in the heliocentric distance range of 0.5- 1.0 AU, many spacecraft in the plane of the sky that are similarly equipped to simultaneously observe density fluctuations and solar wind velocity. Then ask the question: What can these measurements tell us about coronal mass ejections (**CMEs**) observed in white-light measurements?

The preceding circumstances describe radio occultation measurements of the solar corona — measurements that observe a variety of radio propagation and scattering phenomena when a radio source is occulted by the corona. Both natural radio sources and spacecraft radio signals have been used in these experiments, which started in the late 1950s with angular broadening measurements of electron density fluctuations [**Hewish**, 1958; **Vitkevitch**, 1961; Erickson, 1961], before the existence of the solar wind had even been established. Density fluctuations are also observed in measurements of intensity scintillation, phase/Doppler scintillation, and spectral broadening; density in measurements of ranging or time delay and phase; velocity in multiple-station intensity scintillation measurements; and magnetic field and density in Faraday rotation measurements. More recent reviews of these measurements and their results have been given by Watanabe and Schwenn [1989], Bird and Edenhofer [1990], **Coles** [1993], and Hewish [1993].

Since few if any studies of the interplanetary manifestation of CMES based on in situ spacecraft measurements at Earth orbit have been based on signatures of plasma density or solar wind velocity [e.g., Gosling, 1990], the value of radio occultation measurements for investigating CMEs might be questioned. But, the strength in the radio occultation measurements lies in the fact that they probe the same solar wind where white-light CMEs are observed — with ranging actually observing the same plasma parameter as polarization brightness — while providing plasma measurements that are closely related to the solar wind measurements made directly by spacecraft. Radio occultation measurements, therefore, serve as an important and natural bridge between solar and in situ spacecraft measurements beyond 0.3 AU.

In spite of the fragmented and disparate results produced by decades of radio occultation measurements, our knowledge of the corona and its variations based on these unique but limited measurements has been advancing rapidly, and a global picture is emerging [Woo, 1994; 1996a; Woo et al., 1995a]. Variations in the radio occultation measurements that appear different from those of the background solar wind have generally been identified as transients — many of which are produced by CMEs. The purpose of this paper is to summarize recent gains in understanding these coronal transients and their relationship to coronal mass ejections.

## 2. TRANSIENTS IN RADIO OCCULTATION MEASUREMENTS

### a. Early history

Conspicuous coronal transients were detected as soon as space exploration began and spacecraft radio signals were occulted by the solar corona. These early transients — observed in 1968 by Pioneer 6 spectral broadening [Goldstein, 1969] and Faraday rotation measurements [Levy et al., 1969] indicated a corona that was dynamic and rich in structure, a result that may not seem surprising now in light of the recent Yohkoh and SOHO observations. Additional observations of transients followed [Cannon, 1976]. The

Pioneer 6 Faraday rotation transients were interpreted as magnetic bottles [Schatten, 1970], while a major transient — observed later on August 18, 1979 at 13 R. by Voyager 1 measurements of spectral broadening, intensity scintillation, and phase — was identified as an interplanetary shock associated with a solar flare [Woo and Armstrong, 1981; Cane et al., 1982]. The Voyager 1 measurements are notable not only for observing a very fast CME and its associated interplanetary shock, but for providing separate and rare profiles of density, density fluctuations, and solar wind speed, thus showing the relationship between these solar wind parameters. When it was possible to compare spectral broadening and Faraday rotation transients with white-light CMES observed at the same time, a one-to-one correspondence was found between transients and CMES [Bird et al., 1985].

The availability of Doppler tracking measurements by interplanetary spacecraft provided an extensive database for investigating Doppler scintillation transients. Doppler observes the variation in path-integrated density. As in the case of in situ measurements where rms density fluctuations are estimated in a fixed bandwidth (constant sampling rate and interval over which the rms is estimated), Doppler scintillation reflects both solar wind speed and density fluctuations. Spectral broadening does the same, so that for both measurements, profiles of velocity and density fluctuations cannot be deduced unless independent measurements of density fluctuations or solar wind speed are available (e.g., intensity scintillation as in the case of the August 18, 1979 shock observed by Voyager 1 [Woo and Armstrong, 1981]).

When the Doppler scintillation transients were combined with white-light measurements of CMES, speed profiles of interplanetary shocks as a function of heliocentric distance were obtained [Woo et al., 1985]. The frequency of occurrence of the Doppler scintillation transients and its variation over a solar cycle were found to be similar to that of CMES observed in white-light measurements [Woo, 1993], reinforcing the notion based on individual comparisons between CMES and spectral broadening transients [Woo et al., 1982; Bird et al., 1985; Woo et al., 1985] that CMES and Doppler scintillation transients

were different manifestations of the same physical phenomenon. A comparison within situ plasma measurements showed that there was a near one-to-one correspondence between Doppler scintillation transients and interplanetary shocks over a limited 3-month period in 1981-1982 [Woo and Schwenn, 1991]. Since fast CMES produce interplanetary shocks, this result is consistent with the close association between CMES and shocks found in comparisons of white-light and in situ plasma measurements [Sheeley et al., 1985].

#### b. Coronal streamers

A striking pattern of 1984 Pioneer Venus Orbiter (PVO) Doppler scintillation transients was revealed when they were compared with synoptic maps of solar wind parameters based on 6-month averages of direct observations by IMP 8 at 1 AU and PVO at the orbit of Venus [Woo and Gazis, 1993]. Although transients were present in the high density slow solar wind associated with the streamer belt — some of which represented CMES observed by the Solwind white-light coronagraph — the PVO Doppler scintillation transients were conspicuously absent in the low density fast wind associated with coronal holes. Subsequent studies based on Doppler scintillation measurements of the heliospheric current sheet conducted when CMES were not present [Woo et al., 1995a, b] demonstrated that transients also represented the passage of radially expanding coronal streamer stalks observed in white-light coronagraph measurements. These streamer stalks, which measure  $1\text{-}2^\circ$  in angular size and rotate with the Sun, cross the radio path in a couple of hours. The enhanced filamentary structures that comprise the streamer stalk give rise to the observed scintillation transient. It is now clear that those 1984 PVO transients associated with the peaks in density observed in the synoptic maps were most likely coronal streamers, and that the striking PVO scintillation pattern was another manifestation of the close association of CMES and coronal streamers observed in white-light measurements [Hundhausen, 1993].

As in the case of a single spacecraft making in situ measurements during a brief encounter with the Sun, occultation measurements cannot always unambiguously

distinguish between spatial and temporal variations. Still, the interpretation of prominent 2-hour long Doppler scintillation transients in terms of coronal streamers rotating across the radio path was not anticipated. Streamer passage has now been observed in ranging measurements of path-integrated density [Woo et al., 1995b] as well as the electron density spectra inferred from phase scintillation and spectral broadening measurements [Woo and Habbal, 1996], the latter result demonstrating that the small-scale filamentary structures within the streamer stalks are not only stronger but also finer than those in the fast wind associated with coronal holes. Most surprising, however, has been the tracing of the three 1968 Pioneer 6 Faraday rotation and spectral broadening transients to streamer stalk passages as well [Woo, 1996d]. The long delayed streamer identification of the Pioneer 6 transients raises confidence in the general interpretation and usefulness of Faraday rotation transients, while the reversal of magnetic field polarity deduced from them provides observational evidence confirming what has previously only been inferred from modeling [Pneuman and Kopp, 1971] — that streamers observed in white-light measurements are the manifestation of the heliospheric current sheet.

### 3. CORONAL MASS EJECTIONS

#### a. Density and density fluctuations

Simultaneous radio occultation and white-light coronagraph measurements of CMES are crucial not only for establishing the association between transient and CME, but also for understanding the relationship between radio and white-light measurements. Comparison of Helios 2 spectral broadening measurements near 5 R. with Solwind white-light coronagraph measurements of a CME observed on October 24, 1979 showed that the leading edge of the CME did not coincide with the start of the spectral broadening transient, but trailed it [Woo et al., 1982]. Enhanced density and density fluctuations are produced in the compressed plasma ahead of a CME whether or not the CME is moving fast enough to generate an interplanetary shock. Spectral broadening detects the disturbed plasma first

because it is more sensitive to plasma changes than the white-light measurements. But even more important is the fact that spectral broadening senses density fluctuations while white-light observes density, and density fluctuations are enhanced by a factor that is significantly higher than that of density. This dramatic difference between enhanced density and density fluctuations is clearly apparent in the Voyager 1 phase (sensing density) and spectral broadening measurements of the August 18, 1979 interplanetary shock [Woo and Armstrong, 1981], and accounts for why spectral broadening and Doppler scintillation have been more useful for detecting CMES than ranging or phase measurements [Bird and Edenhofer, 1990]. These results indicate that had the Solwind white-light measurements been as sensitive as the Voyager 1 phase measurements, and their spatial resolution high enough, the leading edge of the October 24 CME would have been faint but its detection would have coincided with that of the Helios 2 spectral broadening transient.

Another example of the detection of spectral broadening enhancement beyond the CME boundary is that by Helios 2 of a northern CME observed by Solwind on November 15/16, 1979 near 8 R. [Bird et al., 1985]. A southern CME observed later by Helios 2 near 7 R. is interesting in that the observed spectral broadening bandwidth rises and falls as the CME advances and crosses the Helios 2 radio path. This is consistent with the Voyager 1 measurements of the August 18, 1979 shock showing that spectral broadening bandwidth follows the variation of phase or path-integrated density, and indicating that density fluctuations are roughly proportional to density.

Although there is evolution of the low-latitude solar wind with heliocentric distance, the differences between density and density fluctuations are still evident from direct density measurements at 1 AU. Shown in Fig. 1 are the levels of mean density  $n$ , density fluctuations  $\Delta n$  and fractional density fluctuations  $\Delta n/n$  for various types of solar wind flow compared to those in coronal holes based on 5-rein ISEE 3 solar wind measurements averaged over one hour [Huddleston et al., 1995]. Transient flows from 'CMEs' were identified on the basis of counterstreaming superthermal electrons by Gosling et al. [1987],

and/or the detection of enhanced helium abundance. Hereafter, apostrophes will be used to distinguish 'CMES' identified in this fashion from those observed in the white-light measurements. Interaction regions are the regions between interplanetary shocks and the leading edges of the 'CME' driver gas that follow them, The plasma sheet encompasses the heliospheric current sheet [Winterhalter et al., 1994] and appears to coincide with the streamer stalks detected in Doppler scintillation measurements and discussed earlier [Bavassano et al., 1996].

Although there is little difference in  $n$ ,  $A_n$  and  $A_n/n$  between coronal hole and interstream regions, there are large variations especially in  $A_n$  between the various types of solar wind flow. Consistent with the radio occultation measurements of the August 18, 1979 shock in the solar corona, density and density fluctuations are enhanced in the compressed plasma ahead of the 'CME' (interaction region) as well as within the 'CME', but the enhancement factor of the density fluctuations is significantly higher than that of density. Fig. 1 also shows that there is considerable difference in the level of density fluctuations between 'CME and interaction region. Individual time series of the ISEE 3 solar wind measurements across 'CMES' [see e.g., Gosling, 1990] often show changes in density fluctuations that coincide with the 'CME boundaries, suggesting that density fluctuations may be a characteristic distinguishing the 'CME' plasma.

The results in Fig. 1 illustrate why radio occultation measurements that sense density fluctuations — angular broadening, spectral broadening, intensity and phase/Doppler scintillation — are more effective in distinguishing different solar wind flows than those detecting density, i.e., ranging and phase measurements. Although the different occultation measurements responding to density fluctuations may sense varying and different frequency ranges, the density fluctuations in streamer stalks (plasma sheet), fast wind associated with coronal holes, and flows associated with CMES appear to be wideband [Woo and Armstrong, 1981; Woo et al., 1985; Woo and Armstrong, 1992; Woo and Habbal, 1997], so that similar differences are exhibited in all of the observations.

## b. Magnetic field

As seen in the case of coronal streamers, Faraday rotation observations are unique amongst radio occultation measurements because they respond to magnetic field in addition to density, making it possible to probe the magnetic field. A linearly polarized radio wave propagating through a magnetized plasma as the solar corona will display a rotation in its plane of polarization by an angle  $\Delta\Psi$ :

$$\Delta\Psi = \frac{e^3}{2\pi m_e^2 c^2 f^2} \int n_e \mathbf{B} \cdot d\mathbf{s} \quad (1)$$

where  $n_e$  is electron density,  $B$  the coronal magnetic field,  $d\mathbf{s}$  the incremental path length,  $f$  radio frequency,  $e$  electronic charge,  $m$  electron mass, and  $c$  the speed of light. The angle of rotation is positive when the magnetic field has a component in the direction of radio propagation.

Unfortunately, unraveling Faraday rotation measurements, especially when separate measurements of density are not available, can be very difficult. The interpretation is not unique because different combinations of magnetic field structure and electron density can produce the same net polarization rotation. For instance, in the case of the Pioneer 6 Faraday rotation measurements of a coronal streamer, the observed Faraday rotation throughout the transient was of one sign, suggesting that the magnetic field was **unipolar** [Bird et al., 1985], when in fact there was a polarity reversal in magnetic field [Woo, 1996d]. The situation with rotating streamers is of course unusual. In the case of interplanetary disturbances propagating outward from the Sun, field reversals are more likely to be manifested as sign changes in Faraday rotation.

Although there have only been a few cases of simultaneous spectral broadening and Faraday rotation measurements of white-light CMES, and the data have been far from complete even in those few cases, the comparisons have been invaluable. Fig. 2 is

reproduced from Bird and Edenhofer [1990], showing the Solwind difference images and the corresponding *Helios* time series of spectral broadening bandwidth and Faraday rotation for the October 24, 1979 CME observed on the west limb and mentioned earlier. Additional Solwind images for later times are shown in Bird et al. [1985]. A finer time resolution (2-min integration time) version of the spectral broadening time series in Fig. 2 is given in Fig. 3 of Woo et al. [1982] and affords a better comparison. The leading edge (LE) and a following bright core (BC) were two features that were tracked by Solwind during their radial expansion, giving estimated projected velocities of  $160 \pm 50$  km/s and  $120 \pm 40$  km/s for the leading edge and bright core, respectively. The start of the spectral broadening transient is marked SB, while the estimated arrival times at the *Helios* radio path of the leading edge and bright core by the vertical dashed lines. The widths of the boxes LE and BC indicate the estimated errors of these arrival times.

Like the August 18, 1979 shock, the time history of spectral broadening of the October 24 CME shows two enhanced regions. As discussed earlier, the first region represents the compressed plasma detected ahead of the leading edge of the white-light CME. Enhancement in the second region is at a lower level than in the first. Since spectral broadening bandwidth responds to both density fluctuations and solar wind velocity, part of the lowering reflects the slower speed of the bright core. The start of the second region of enhancement coincides roughly with the arrival of the bright core (indicating enhanced density), after which Faraday rotation changes sign several times, indicating probable polarity reversals in magnetic field. Strictly speaking, the sign change in Faraday rotation applies to the combination of background solar wind and CME, but we will assume that the CME contribution is dominant. However, when the background is removed, the locations of the polarity reversals do not appear to change significantly [Bird et al., 1985].

Further evidence for reversals taking place behind the compressed plasma detected by spectral broadening are found in the October 23, 1979 and November 16, 1979 Faraday rotation transients reported by Bird et al. [1985]. The time histories of spectral broadening

and Faraday rotation of these two CMES are reproduced in Figs. 3 and 4, respectively. Like the October 24, 1979 CME and the August 18, 1979 interplanetary shock, the profiles of spectral broadening show a distinct second region of enhanced bandwidth behind the first. Although white-light measurements are not available for the November 16 transient, the white-light measurements of the October 24 transient indicate that the bright core arrives at the Helios 2 radio path at about 1330 UT, near the start of the second spectral broadening enhancement. Contrary to the October 24 CME, the October 23 and November 16 transients exhibit single rather than multiple polarity reversals of magnetic field behind the compressed plasma ahead of the CME, indicating that polarity reversals are absent from their cores. The time histories of spectral broadening and Faraday rotation of the October 23 CME reinforce the notion that density rather than magnetic field variation appears to be dominating the Faraday transient after the polarity reversal. The apparent **anticorrelation** of spectral broadening and Faraday rotation after 1330 UT suggests that density fluctuations are varying in step with density, as would be expected if density fluctuations are proportional to density.

Single and multiple reversals in magnetic field polarity are also a common feature behind the enhanced density fluctuations representing the compressed plasma ahead of 'CMES' observed at 1 AU in solar wind measurements [Gosling, 1990]. They can be interpreted as representing the deflection of the ambient plasma ahead of the 'CME' or the draping of the ambient magnetic field around the front of the 'CME' {Gosling and McComas, 1987}. Gosling [1990] has shown that in 30% of all 'CMES' observed at 1 AU, coherent internal field rotations within the 'CMES' that are characteristic of magnetic flux ropes are observed, and these would also cause polarity reversals.

The polarity reversals detected in the white-light CMES by the Faraday rotation measurements are obviously closely related to those observed in the 'CMES.' Combining the results from spectral broadening, Faraday rotation, phase, white-light, and in situ plasma measurements, the following CME features and their interpretation seem to be

emerging, Two regions of enhanced spectral broadening appear common to CMEs. The first represents the enhanced density fluctuations of the compressed plasma ahead of the CME, while the second the bright core of the CME. This interpretation is consistent with the fact that, in the case of the November 15/16 CME discussed earlier, since the bright core of the CME did not cross the Helios 2 radio path, only one enhanced region. Polarity reversals caused by deflection of the magnetic field by the CME occur behind the compressed plasma. As in the case of 'CMEs' observed by in situ measurements, polarity reversals are not always observed in the bright cores of CMEs. CMES with multiple reversals in the core of the CME are suggestive of large internal field rotations, magnetic flux ropes, and magnetic cloud [Burlaga et al., 1982]. When comparisons between white-light and direct spacecraft measurements of the same CME event are made, it is clear that the availability of magnetic field measurements of the white-light CME provided by Faraday rotation would be extremely useful.

Although highly uncertain, magnetic field estimates based on the Faraday rotation measurements also suggest that the longitudinal component of the magnetic field during the transient could be higher than the pre-transient ambient radial magnetic field [Bird et al., 1985]. This is also consistent with the magnetic field measurements of 'CMEs' at 1 AU.

#### 4. MEASUREMENTS BEYOND 0.5 AU

The emphasis in this paper has been on radio occultation measurements of the corona. Meter wavelength intensity scintillation observations (intensity scintillation is often referred to as IPS for interplanetary scintillation) have yielded extensive measurements of density fluctuations and solar wind velocity in the heliocentric distance range of 0.3- 1.0 AU, and are notable for providing maps of solar wind velocity and enhanced scintillation representing interplanetary disturbances in the plane of the sky. Meter wavelength IPS measurements have been discussed elsewhere [Houminer, 1977; Kakinuma, 1977;

Watanabe and Schwenn, 1989; Hewish, 1993; Manoharan, 1996], and only a few relevant comments based on the results discussed here will be made.

The enhanced scintillation observed in meter wavelength IPS measurements reflect both propagating interplanetary disturbances and corotating solar wind features, which are sometimes more difficult to distinguish beyond 0.5 AU because of radial evolution and path-integrated effects. As in the case of scintillation measurements close to the Sun, and as is apparent from direct measurements of 'CMEs' at 1 AU, the compressed plasma ahead of the 'CME' as well as the turbulence within the 'CME' give rise to the enhanced scintillation in propagating interplanetary disturbances. Searches for coronal streamers based on IPS measurements beyond 0.5 AU have not been successful [Houminer and Gallagher, 1993], and corotating high speed streams (corotating interaction regions) have generally been identified as the corotating enhanced scintillation feature. However, it is clear from tracking coronal streamers to 1 AU [Woo et al., 1996], and from in situ measurements at 1 AU [Huddleston et al., 1995], that the corotating enhanced IPS features observed beyond 0.5 AU often include both coronal streamers and the compressed plasma at the leading edges of high speed streams (compare profiles given in Ananthakrishnan et al. [1980] with those in Huddleston et al. [1995]).

Fractional density fluctuations has relevance to the use of density fluctuations observed in IPS as a proxy for density [Tappin, 1986]. Although the fluctuation frequencies are not exactly the same, the results in Fig. 1 that are based on direct measurements suggest that this is a reasonable assumption for measurements near 1 AU;  $n/n_0$  does not change significantly across the different types of solar wind, and especially between interaction region and 'CME.'

Some studies have suggested that coronal holes might be the source of interplanetary disturbances detected in IPS measurements [Hewish et al., 1985; Bravo et al., 1991]. The connection between these disturbances and their source region on the Sun is best investigated with measurements closer to the Sun. The conspicuous absence of near-Sun

Doppler scintillation transients from coronal hole regions [Woo and Gazis, 1993] demonstrates that coronal hole regions cannot be a major source of these disturbances.

Finally, the difference between density and density fluctuations in the solar wind appears to be one of the reasons why meter wavelength IPS measurements have been more effective in detecting interplanetary disturbances and corotating streams beyond 0,5 AU than meter wavelength ranging (group delay) measurements [Croft, 1979].

## 5. SUMMARY AND DISCUSSION

Radio occultation measurements of the solar corona have been conducted for a long time. However, because they are made during conjunctions, the encounters with the corona have generally been brief. Furthermore, the observations, usually limited to observing only one or two of the radio phenomena at a time, have also been discontinuous. Until now, the synthesis of these fragmented results has not been possible because of the limited plasma parameters observed, together with the general complication of the solar wind variations. Key factors that have led to the recent progress in the morphology of the dynamic and structured solar corona include a better understanding of the: (1) the nature of the density fluctuations [Woo, 1996b], (2) the extent to which spatial structures permeate the corona [Woo, 1995; 1996a, b, c], (3) the relationship between the observations of disparate radio propagation and scattering phenomena [Woo, 1996b; Woo and Habbal, 1996], and (4) the relationship between radio occultation, white-light and in situ fields and particles measurements.

A major development in the understanding of the probing of the solar corona by radio occultation measurements has been the realization that although density fluctuations represent a relatively small fraction of the mean density, the variation of density fluctuations in different solar wind flows is significantly greater than that of density [Woo, 1996a]. Thus, radio occultation measurements sensing density fluctuations — a parameter that has not usually received much attention in solar wind studies based on in situ measurements —

have been more effective in probing the near-Sun solar wind than those sensing density. The variation of small-scale density fluctuations between coronal holes, streamers and CMES near the Sun is both striking and abrupt, and in spite of evolution with heliocentric distance is still evident in the in situ density measurements at 1 AU. Prominent transients caused by the passage of coronal streamers stem from the enhanced small-scale density variations across the filamentary structures in the stalks of the streamers. Coronal mass ejections produce even more spectacular transients because of the still higher levels of density fluctuations generated in the compressed turbulent plasma ahead of the CME and the high propagation speeds of the CMEs. Measurements that sense density fluctuations, e.g., Doppler scintillation and spectral broadening, detect the transients and establish the context for measurements that sense density and magnetic field. Useful information on magnetic field from Faraday rotation transients have been obtained only after the transients have been established and put into perspective by spectral broadening measurements, leading to the detection of the heliospheric current sheet in streamer stalks, and polarity reversals in magnetic field behind the compressed plasma ahead of CMEs.

In spite of their limitations, radio occultation measurements of CMES complement white-light and in situ plasma measurements of CMES in significant ways. With regard to measuring path-integrated density, ranging is more sensitive than white-light. More importantly, because of the difference between density and density fluctuations, radio occultation measurements responding to density fluctuations are more sensitive to CMES than white-light. Even if the measurements of polarized brightness by a white-light coronagraph were as sensitive and precise as phase measurements, CMES would not appear as conspicuous and prominent as they would in measurements of density fluctuations. By providing information on magnetic field, Faraday rotation complements white-light measurements in a significant way. While complicated to interpret, the recent identification of the coronal streamer signature has improved the usefulness of Faraday rotation measurements. Faraday rotation measurements are particularly important for

investigating CMES, because they are sensitive to magnetic field polarity reversals, and therefore provide clues about their magnetic field topology. Compared with in situ measurements, the plasma parameters observed during radio occultation observations are limited. Still, density fluctuations are a surprisingly useful plasma parameter for investigating CMEs, especially since in situ measurements of CMES will probably not be obtained even during a flyby mission such as Solar Probe.

There have been only a few cases for which radio occultation and white-light measurements of CMES could be compared, and the measurements have been incomplete, but two regions of enhanced density and density fluctuations appear common to CMEs. The first region, representing the compressed plasma ahead of the CME, is present whether or not the CME is traveling fast enough to generate an interplanetary shock, and may be related to forerunners observed in the white-light measurements [Jackson and Hildner, 1973]. Mainly because density fluctuations are enhanced by a significantly higher factor than density, but also because of the lower sensitivity of the white-light measurements, the enhanced density fluctuations are detected before the leading edge of the white-light CME. Reversals in magnetic field polarity, presumably caused by the deflection of the ambient magnetic field by the advancing CME, are found behind the compressed plasma ahead of the CME.

The second region of enhanced density and density fluctuations appears to coincide approximately with the bright core of the CME. As in the case of CMES observed by in situ measurements and identified as counterstreaming sup-thermal electrons events, polarity reversals are not always observed in the bright cores of CMES. While some CMES show no magnetic field polarity reversals in the second region of enhanced density fluctuations, others show multiple reversals that are suggestive of large internal field rotations, magnetic flux ropes, and magnetic cloud.

It is important to fully exploit radio occultation measurements to study CMES near the Sun. Future measurements would be most useful if they yield simultaneous profiles of

density, density fluctuations, solar wind velocity and magnetic field, which means observing different radio phenomena at the same time. The improved understanding of the signatures of coronal mass ejections, streamers, and plumes increases the chances that other coronal features that would also appear as transients in radio occultation measurements could be identified, e.g, soft X-ray jets [Shimojo et al., 1996] or the interplanetary manifestation of soft X-ray bright points. The value of radio occultation measurements increases significantly when conducted with other observations. Current and future NASA missions with which radio occultation measurements of the corona can be conducted include Galileo, Near, Mars Global Surveyor, and Cassini; coordinated observations with SOHO, Yohkoh and direct spacecraft measurements would be especially valuable.

Acknowledgments. It is a pleasure to thank J. Armstrong for many useful discussions. This paper describes research carried out at the Jet Propulsion Laboratory, California Institute of Technology, under a contract with the National Aeronautics and Space Administration.

#### REFERENCES

- Ananthakrishnan, S., W.A. Coles, and J.J. Kaufman, **Microturbulence** in solar wind streams, *J. Geophys. Res.*, 85, 6025–6030, 1980.
- Bavassano, B., R. Woo, R. Bruno, and H. Rosenbauer, The **heliospheric** plasma sheet in near-the-Sun solar wind, paper presented at the *Third Symposium on Solar and Interplanetary Transient Phenomena*, Beijing, China, October 14-18, 1996.
- Bird, M. K., H. Volland, R.A. Howard, M.J. Koomen, D.J. Michels, N.R. Sheeley, Jr., J.W. Armstrong, B.L. Seidel, C.T. Stelzried, and R. Woo, White-light and radio sounding observations of coronal transients, *Solar Phys.*, 98, 341–368, 1985.

- Bird, M. K., and P. Edenhofer, 1990, Remote sensing observations of the solar corona, in *Physics of the Inner Heliosphere, I*, ed. R. Schwenn and E. Marsch, Springer-Verlag, Berlin, 1990.
- Bravo, S., B. Mendoza, and R. Pérez-Enriquez, Coronal holes as sources of large-scale solar wind disturbances and geomagnetic perturbations, *J. Geophys. Res.*, *96*, 5387–5396, 1991.
- Burlaga, L.F., L. Klein, N.R. Sheeley, Jr., D.J. Michels, R.A. Howard, M.J. Koomen, R. Schwenn, and H. Rosenbauer, A magnetic cloud and a coronal mass ejection, *Geophys. Res. Letts.*, *9*, 1317-1320, 1982.
- Cane, H. V., R.G. Stone, and R. Woo, Velocity of the shock generated by a large east limb flare on August 18, 1979, *Geophys. Res. Letts.*, *9*, 897-900, 1982.
- Cannon, A.R., Radio-frequency probing of the solar corona, PhD thesis, 426pp., University of California, Berkeley, 1976.
- Coles, W. A., Scintillation in the solar wind (IPS), in *Wave propagation in random media (Scintillation)*, eds. V. Tatarskii, A. Ishimaru, and V. Zavorotny, 156-168, SPIE, Bellingham, 1993.
- Croft, T. A., A graphical summary of solar wind electron content observations by Pioneer 6,8, and 9, *J. Geophys. Res.*, *84*, 439-449, 1979.
- Erickson, W. C., The radio-wave scattering properties of the solar corona, *Astrophys. J.*, *139*, 1290-1311, 1964.
- Goldstein, R. M., Superior conjunction of Pioneer 6, *Science*, *166*, 598-601, 1969.
- Gosling, J. T., Coronal mass ejections and magnetic flux ropes in interplanetary space, AGU Monograph 58, 343-364, 1990.
- Gosling, J.T., and McComas, D. J., Field line draping about fast coronal mass ejects: A source of strong out-of-the-ecliptic interplanetary magnetic fields, *Geophys. Res. Letts.*, *14*, 355-358, 1987.

- Gosling, J.T., D.N. Baker, S.J. Bame, W.C. Feldman, R.D. Zwickl, and E.J. Smith, Bidirectional solar wind electron heat flux events, *J. Geophys. Res.*, 92,8519-8535, 1987.
- Hewish, A., The scattering of radio waves in the solar corona, *Mon. Not. Roy. Astr. Soc.*, 118, 534-546, 1959.
- Hewish, A., Interplanetary scintillation imaging of disturbances in the solar wind, in *Wave propagation in random media (Scintillation)*, eds. V. Tatarskii, A. Ishimaru, and V. Zavorotny, 261-270, SPIE, Bellingham, 1993.
- Hewish, A., S.J. Tappin, and G.R. Gapper, Origin of strong interplanetary shocks, *Nature*, 314, 137-140, 1985.
- Houminer, Z., Scintillation observations of the interplanetary plasma, in *Study of Traveling Interplanetary Phenomena 1977*, eds. M.A. Shea, D.F. Smart, and S.T. Wu, Reidel, Dordrech, Holland, 119-141, 1977.
- Houminer, Z., and F. Gallagher, A search for coronal streamers near 1 AU using interplanetary scintillation, *Solar Phys.*, 145,359-375, 1993.
- Huddleston, D.E., R. Woo, and M. Neugebauer, Density fluctuations in different types of solar wind flow at 1 AU and comparison with results from Doppler scintillation measurements near the Sun, *J. Geophys. Res.*, 100, 1995 1–19956, 1995.
- Hundhausen, A., Sizes and locations of coronal mass ejections: SMM observations from 1980 and 1984-1989, *J. Geophys. Res.*, 98, 13177-13200, 1993.
- Jackson, B.V., and E. Hildner, Forerunners: Outer rims of solar coronal transients, *Solar Phys.*, 60, 155, 1973.
- Kakinuma, T., Observations of interplanetary scintillations: Solar wind velocity, in *Study of Traveling Interplanetary Phenomena 1977*, eds. M.A. Shea, D.F. Smart, and S.T. Wu, Reidel, Dordrech, Holland, 101-118, 1977.

- Levy, G. S., T. Sate, B.L. Seidel, C.T. Stelzried, J.E. Ohlson, and W.V.T. Rusch, Pioneer 6: Measurement of transient Faraday rotation phenomena observed during solar occultation, *Science*, 166, 596-598, 1969.
- Manoharan, P. K., The origin of interplanetary disturbances, *Geophys. Res. Letts.*, in press.
- Pneuman, G., and R.A. Kopp, Gas-magnetic field interactions in the solar corona, *Solar Phys.*, 18, 258-270, 1971.
- Schatten, K. H., Evidence for a coronal magnetic bottle at 10 solar radii, *Solar Phys.*, 12, 484-491, 1970a.
- Sheeley, N, R., Jr., R.A. Howard, M.J. Koomen, D.J. Michels, R. Schwenn, K.H. Mulhauser, and H. Rosenbauer, Coronal mass ejections and interplanetary shocks, *J. Geophys. Res.*, 90, 163–175 , 1985.
- Shimojo, M., S. Hashimoto, K. Shibata, T. Hirayama, H.H. Hudson, and L.W. Acton, Statistical study of solar X-ray jets observed with the Yohkoh soft X-ray telescope, *Publ. Astron. Sot. Japan*, 48, 123-136, 1996.
- Stelzried, C. T., G.S. Levy, T. Sate, W.V.T. Rusch, J.E. Ohlson, K.H. Schatten, and J.M. Wilcox, The quasi-stationary coronal magnetic field and electron density as determined from a Faraday rotation experiment, *Solar Phys.*, 14,440456, 1970.
- Tappin, S. J., Interplanetary scintillation and plasma density, *Planet. Space Sci.*, 34, 93-97, 1986.
- Vitkevitch, V.V., Radio astronomical observations of moving plasma clouds in the solar supercorona, *Sov. Astron.*, 4, 897–903, 1961.
- Watanabe, T., and R. Schwenn, Large-scale propagation properties of interplanetary disturbances revealed from IPS and spacecraft observations, *Space Sci. Rev.*, 51, 147-173, 1989.
- Winterhalter, D., E.J. Smith, M.E. Burton, N. Murphy, and D.J. McComas, The heliospheric plasma sheet, *J. Geophys. Res.*, 99, 6667-6680, 1994.

- Woo, R., Solar cycle variation of interplanetary disturbances observed as Doppler scintillation transients, *J. Geophys. Res.*, 98, 18999-19004, 1993.
- Woo, R., in *Third SOHO Workshop Solar Dynamic Phenomena and Solar Wind Consequences*, ESA SP-373, 239-248, 1994.
- Woo, R., Solar wind speed structure in the inner corona at 3–12  $R_{\odot}$ , *Geophys. Res. Letts.*, 22, 1393-1396, 1995.
- Woo, R., Coronal structures observed by radio propagation measurements, in *Proc. Solar Wind Eight*, ed. D. Winterhalter, J. Gosling, S.R. Habbal, W. Kurth, and M. Neugebauer (New York: AIP), 1996a.
- Woo, R., Kilometre-scale structures in the Sun's corona, *Nature*, 379, 321-322, 1996b.
- Woo, R., Detection of low-latitude plumes in the outer corona by Ulysses radio ranging measurements, *Astrophys. J.*, 464, L95–L98, 1996c.
- Woo, R., Evidence for the reversal of magnetic field polarity in coronal streamers, *Geophys. Res. Letts.*, submitted, 1996d.
- Woo, R., and J.W. Armstrong, Measurements of a solar flare-generated shock wave at 13.1  $R_{\odot}$ , *Nature*, 292, 608–610, 1981.
- Woo, R., and J.W. Armstrong, Observations of the electron density spectrum near the Sun during spectral broadening transients, in *Solar Wind Seven*, eds. E. Marsch and R. Schwenn, Pergamon Press, Oxford, 583–586, 1992.
- Woo, R., and P. Gazis, Large-scale solar-wind structure near the Sun detected by Doppler scintillation, *Nature*, 366, 543–545, 1993.
- Woo, R., and S.R. Habbal, Finest filamentary structures of the inner corona in the slow and fast solar wind, *Astrophys. J.*, in press, 1996.
- Woo, R., and R. Schwenn, Comparison of Doppler scintillation and in situ spacecraft plasma measurements of interplanetary disturbances, *J. Geophys. Res.*, 96, 21227–21244, 1991.

- Woo, R., J. W. Armstrong, N.R. Sheeley, Jr., R.A. Howard, D.J. Michels, and M.J. Koomen, Simultaneous radio scattering and white light observations of a coronal transient, *Nature*, 300, 157-159, 1982.
- Woo, R., J.W. Armstrong, N.R. Sheeley, Jr., R.A. Howard, M.J. Koomen, and D.J. Michels, Doppler scintillation observations of interplanetary shocks within 0.3 AU, *J. Geophys. Res.*, 90, 154-162, 1985.
- Woo, R., J.W. Armstrong, and P.R. Gazis, Doppler scintillation measurements of the heliospheric current sheet and coronal streamers close to the Sun, *Space Sci. Rev.*, 72, 223-228, 1995a.
- Woo, R., J.W. Armstrong, M.K. Bird, and M. Pätzold, Fine-scale filamentary structure in coronal streamers, *Astrophys. J.*, 449, L91-L94, 1995b.

## FIGURE CAPTIONS

Fig. 1 Ratios of mean density  $n$ , density fluctuations  $\Delta n$ , and fractional density fluctuations  $\Delta n/n$  for various solar wind flow to the values in coronal hole flow (from Huddleston et al. (1995]).

Fig. 2 Time histories of Faraday rotation (**FR**) and spectral broadening (**SB**), and Solwind white-light coronagraph images of the October 24, 1979 **CME** (reproduced from Bird and Edenhofer [1990]). The three Solwind difference images at the top show the geometrical relationship between the **CME** and the apparent position of **Helios 2** off the west limb of the Sun indicated by the white dots.

Fig. 3 Time histories of Faraday rotation (**FR**) and spectral broadening (**SB**) for the October 23, 1979 **CME** observed by the Solwind white-light coronagraph (reproduced from Bird et al. [1985]).

Fig. 4 Time histories of Faraday rotation (**FR**) and spectral broadening (**SB**) for the November 16, 1979 **CME** observed by the Solwind white-light coronagraph (reproduced from Bird et al. [1985]).

Difference Images : 24 October 1979

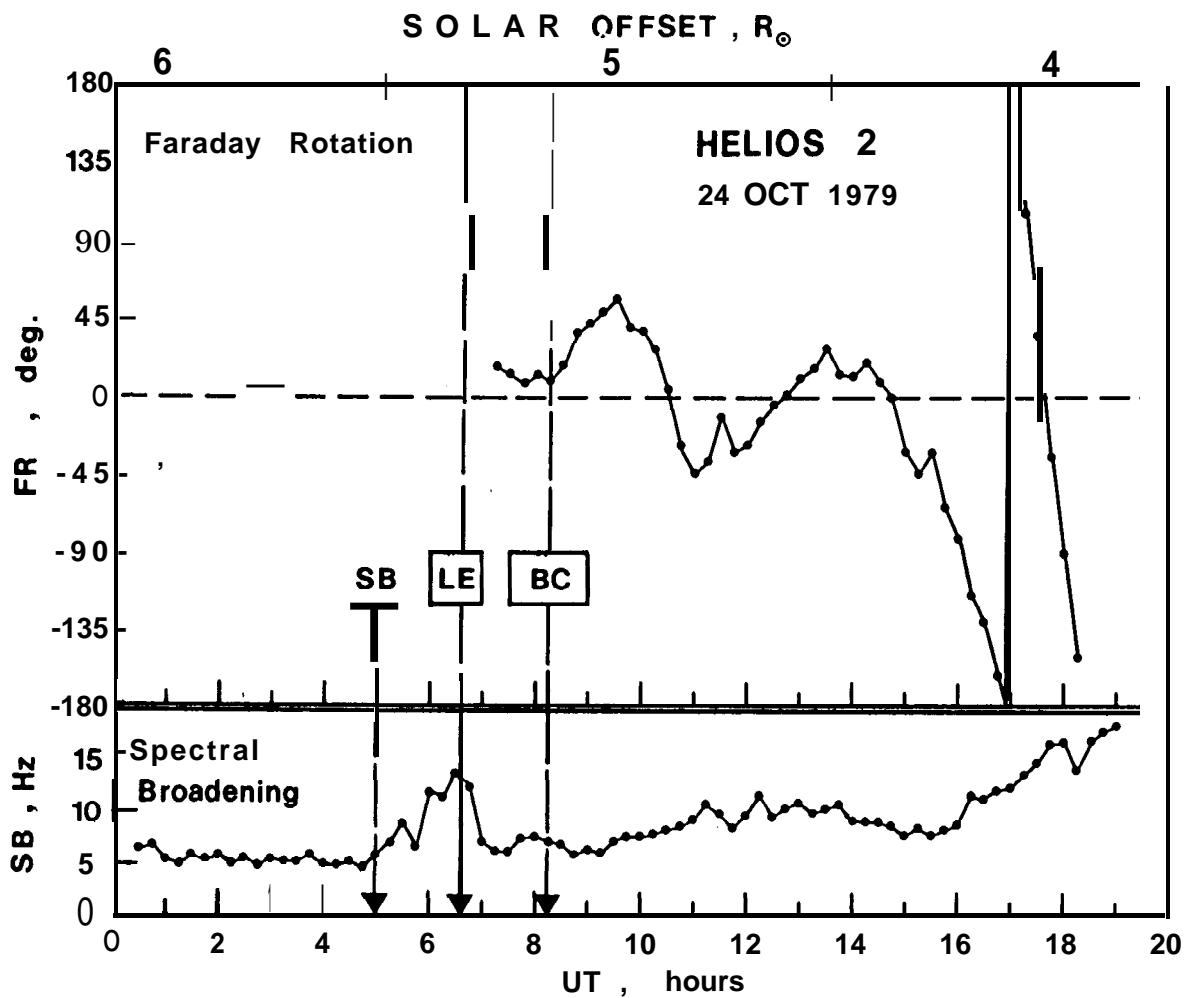
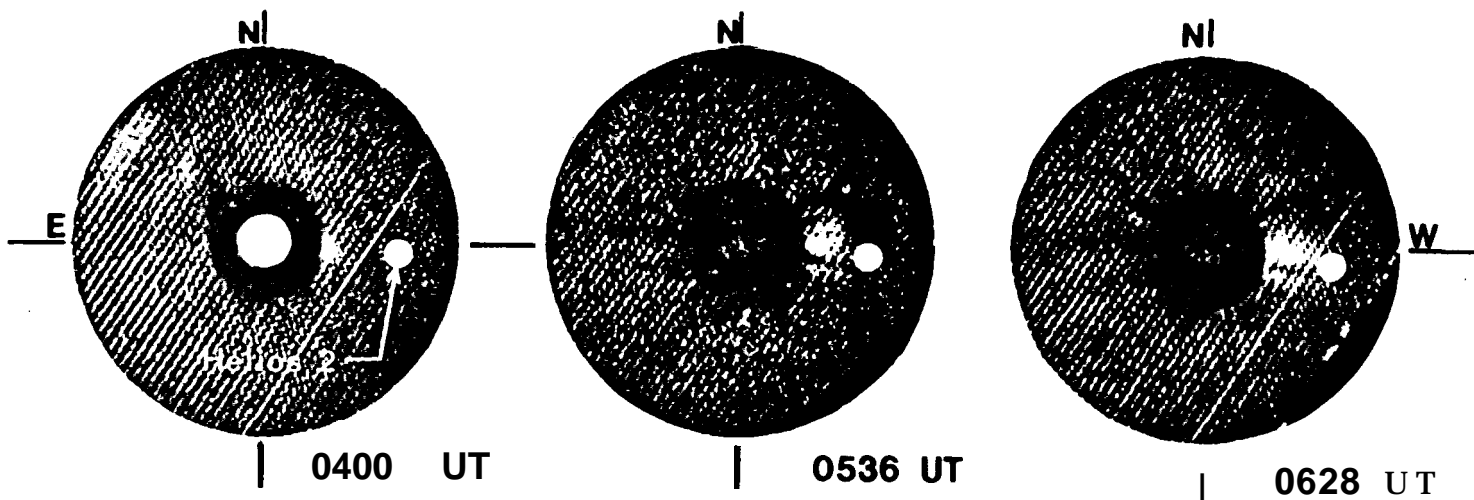


Fig. 1

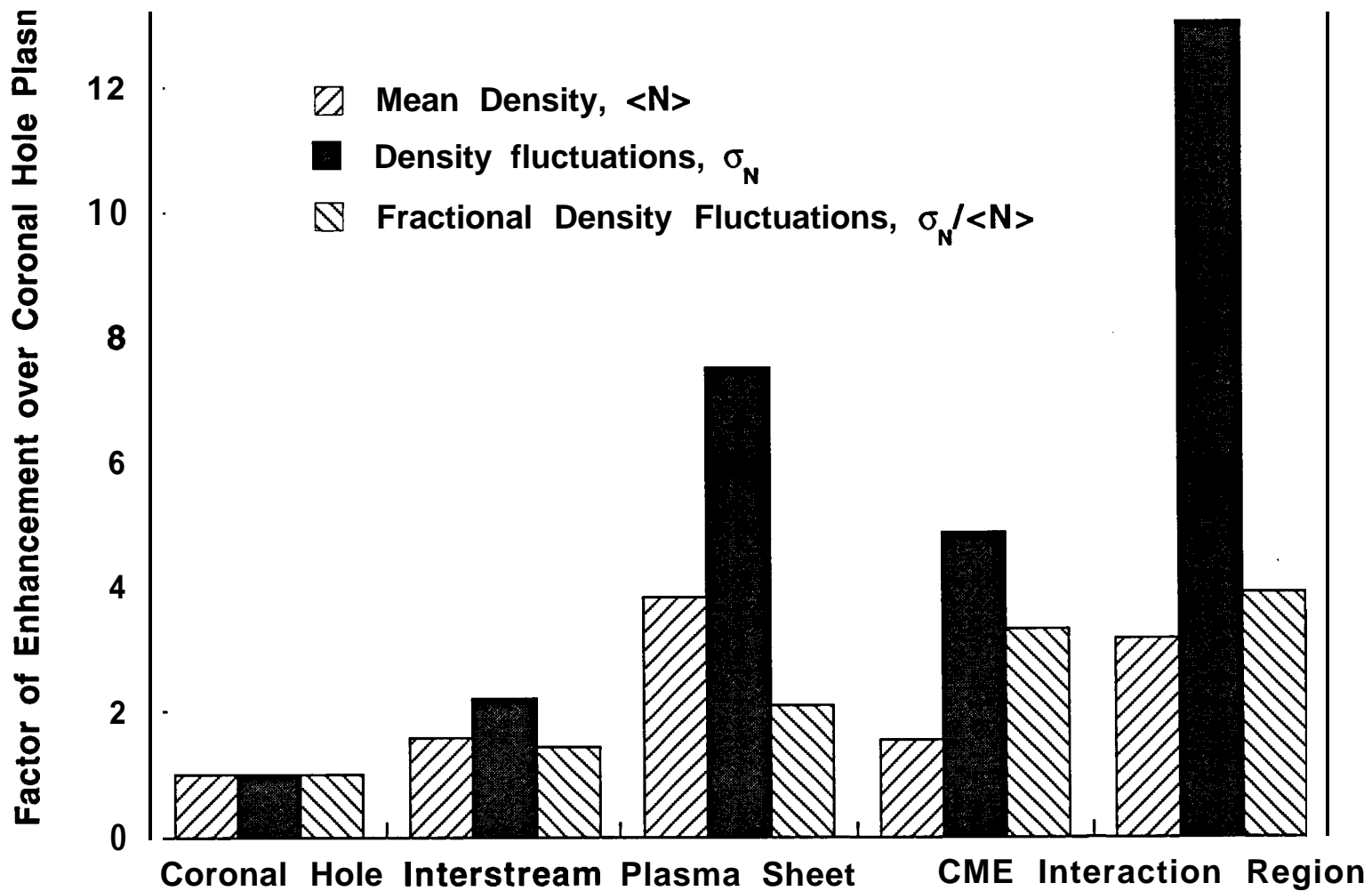
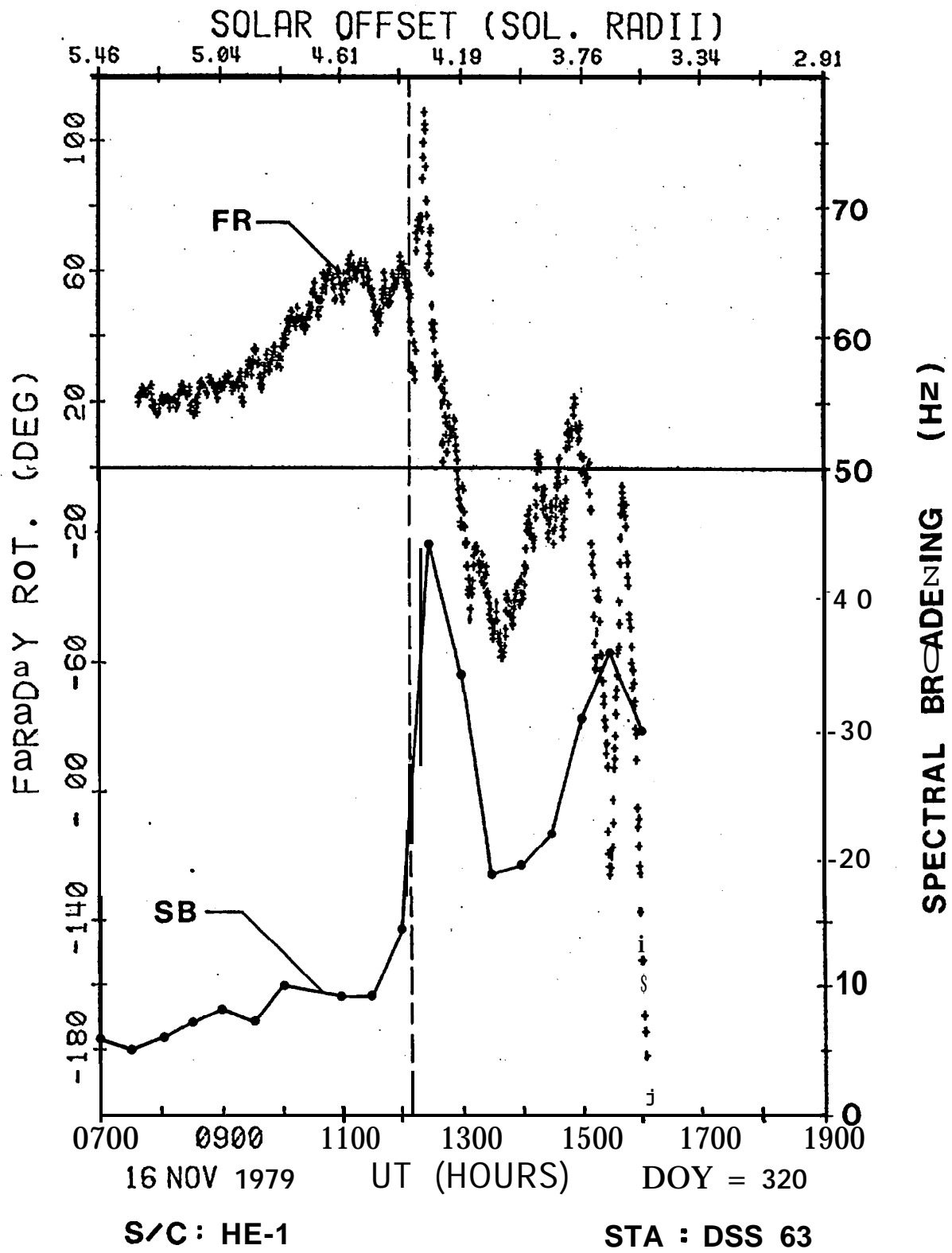


Fig. 2





1200